Carnegie Observatories Astrophysics Series, Vol. 4:
Origin and Evolution of the Elements, 2004
ed. A. McWilliam and M. Rauch (Cambridge: Cambridge Univ. Press)

Interstellar Atomic Abundances

EDWARD B. JENKINS
Princeton University Observatory

Abstract

A broad array of interstellar absorption features that appear in the ultraviolet spectra of bright sources allows us to measure the abundances and ionization states of many important heavy elements that exist as free atoms in the interstellar medium. By comparing these abundances with reference values in the Sun, we find that some elements have abundances relative to hydrogen that are approximately consistent with their respective solar values, while others are depleted by factors that range from a few up to around 1000. These depletions are caused by the atoms condensing into solid form onto dust grains. Their strengths are governed by the volatility of compounds that are produced, together with the densities and velocities of the gas clouds. We may characterize the depletion trends in terms of a limited set of parameters; ones derived here are based on measurements of 15 elements toward 144 stars with known values of $N(\text{H I})$ and $N(\text{H}_2)$. In turn, these parameters may be applied to studies of the production, destruction, and composition of the dust grains. The interpretations must be done with care, however, since in some cases deviations from the classical assumptions about missing atoms in unseen ionization stages can create significant errors. Our experience with the disk of our Galaxy offers important lessons for properly unravelling results for more distant systems, such as high- and intermediate-velocity clouds in the Galactic halo, material in the Magellanic Stream and Magellanic Clouds, and otherwise invisible gas systems at large redshifts (detected by absorption features in quasar spectra). Inferences about the total (gas plus dust) abundances of such systems offer meaningful information on their origins and/or chemical evolution.

1.1 Introduction

For those who study the interstellar medium (ISM), the manifold states that atoms can assume in space are both a benefit and a hindrance. On the favorable side, the apportionments of atoms in various ionization stages and the fractions that become bound in molecular compounds (including solids) reveal the outcomes of fundamental processes that arise from various physical and chemical influences, and these, in turn, disclose the nature of nearby objects or conditions that created these circumstances. Conversely, if it turns out that we have a poor understanding of the fractions of atoms that exist in unseen states, we are hampered in our ability to gauge the relative total abundances of different elements. These two considerations underscore the importance of our mastering the principles that govern how the atoms are subdivided into different states within environments that range from the local part of our Galaxy to the most distant gas systems that we can detect in the Universe. A major theme in this article will be to cover the underlying principles of this topic.

Viewing atomic species by their absorption features in the spectra of background continuum sources, such as stars or quasars, offers the simplicity of not having to understand the details of how the atoms are excited, as we must do if we are observing emission lines arising from collisional excitation or recombination. Moreover, the radiative transfer of absorption features in the optical and ultraviolet regions is straightforward, since the attenuation of light follows a simple exponential absorption law. Studies of absorption lines have revealed a broad assortment of findings on the state and composition of interstellar gases, and we review here many of these conclusions.

At this point, it is appropriate to digress and offer a brief historical perspective. The papers in this volume arose from one of four symposia that celebrated the founding of the Carnegie Observatories exactly 100 years ago. We may reflect on the fact that some two years after that event, Hartmann (1904) reported that stationary Ca II lines in the spectrum of the spectroscopic binary δ Ori arose from the intervening medium, rather than from the atmospheres of the stars. As with many important discoveries, doubts about the interpretation remained (Young 1922), but eventually the interstellar nature of these features was firmly established (Plaskett & Pearce 1933). There soon followed large surveys of interstellar lines, with Carnegie astronomers playing an important role in the process (Merrill et al. 1937; Adams 1949). Nowadays, modern echelle spectrographs with very high resolving powers show exquisite recordings of the complex superpositions of narrow velocity features, and these data allow one to study either weak features or those arising from very small parcels of gas along the line of sight to the target stars (e.g., Blades, Wynne-Jones, & Wayte 1980; Welsh, Vedder, & Vallerga 1990; Welty, Hobbs, & Kulkarni 1994; Barlow et al. 1995; Crane, Lambert, & Sheffer, 1995; Welty, Morton, & Hobbs 1996; Crawford 2001; Welty & Hobbs 2001; Knauth, Federman, & Lambert 2003; Welty, Hobbs, & Morton 2003).

Against the backdrop of almost 100 years of studies of the interstellar medium using absorption features in the visible part of the spectrum, we celebrate yet another anniversary. Some 30 years ago the first papers describing results from the *Copernicus* satellite (Rogerson et al. 1973a), launched in 1972, demonstrated the extraordinary utility of using the ultraviolet part of the spectrum to study a vast array of features arising from important interstellar atomic constituents (Morton et al. 1973; Rogerson et al. 1973b), along with our first insights on the excitation and widespread presence of molecular hydrogen (Spitzer et al. 1973; Spitzer & Cochran 1973). Spitzer & Jenkins (1975) reviewed many of the principal conclusions that came from this initial venture into the ultraviolet.

Additional inferences on the nature of the ISM arose from the *International Ultraviolet Explorer (IUE)* (Kondo et al. 1987), which bridged the *Copernicus* era and that of the *Hubble Space Telescope (HST)*, launched in 1990. *HST* still functions as a premier facility for gathering useful observations of interstellar absorption lines through the use of a new instrument, the Space Telescope Imaging Spectrograph (STIS) that was installed in 1997 (Kimble et al. 1998; Woodgate et al. 1998). A comprehensive review of the findings on interstellar abundances gathered from *HST* up to 1996 [using a first-generation spectrograph, the Goddard High-Resolution Spectrograph (GHRS)], has been written by Savage & Sembach (1996). Finally, the *Far Ultraviolet Spectroscopic Explorer (FUSE)* (Moos et al. 2000) offers an opportunity to revisit the spectral region $912-1185$ Å with high sensitivity, a band that has been mostly inaccessible since the days of *Copernicus*.

In parallel with investigations of the Galactic ISM using observatories in Earth orbit, large-aperture telescopes on the ground have allowed us to study absorptions by the same UV transitions arising from gaseous material at very large redshifts. Much of the progress in understanding the abundances in these distant systems has drawn upon lessons learned from studies of Galactic material, where we have better insights on the fundamental abundance patterns (from the Sun and stars) and the physical conditions. Recent reviews by Pettini (2003) and Calura et al. (2004) summarize the current state of many of the conclusions on highly redshifted systems that have arisen from such studies.

In the sections that follow, we will explore how the apparent abundances of elements are altered by the effects of ionization and depletion onto dust grains. We bypass discussions of the techniques employed to study the absorption features. The reader is referred to a number of papers that cover some key points on the methodology of this type of research (Cowie & Songaila 1986; Jenkins 1986, 1996; Savage & Sembach 1991; Sembach & Savage 1992), plus a list of possible pitfalls in its conduct (Jenkins 1987).

1.2 Ionization Corrections

Of all the species that have absorption features in the visible part of the spectrum, Ti II is the only one that represents an element in its favored stage of ionization within H I regions. The remaining species, Li I, Ca I, Ca II, Na I, and K I all have an ionization potential less than that of H I, with the consequence that they are mostly ionized to higher stages by UV starlight photons that can easily penetrate the regions. One may attempt to derive the gas-phase abundance of an element X from solutions of the ionization equilibrium equation involving the element's ionization rate $\Gamma(X)$ from starlight photons, balanced against its rate of recombination governed by the rate coefficients $\alpha(X,e)$ with free electrons and $\alpha(X,g)$ with negatively charged or neutral, very small dust grains [at a rate that is normalized to the hydrogen density $n(\mathrm{H})$*] (Weingartner & Draine 2001). That is, in principle the balance

$$n(X^0)\Gamma(X) = n(X^+)[\alpha(X,e)n(e) + \alpha(X,g)n(\mathrm{H})] \qquad (1.1)$$

may be solved to yield a total abundance of X if the parameters are well defined. If the local values of $\Gamma(X)$ and the electron and hydrogen densities $n(e)$ and $n(\mathrm{H})$ are poorly known, it is still possible to take Equation 1.1 for element X and divide it by that for another element (Y) to derive a relative abundance of the two (X/Y). While this may seem to be an attractive solution for studying abundance trends, recent comparisons made by Welty, Hobbs & Morton (2003) indicate that different elements showing features in the ultraviolet show mutually inconsistent values for the ratios of adjacent ionization stages when Equation 1.1 is invoked in the respective cases. These disparities may arise from either errors in the atomic constants or, perhaps in some cases, from rapid changes in conditions that prevent the equilibria from being fully established. Until these effects are better understood, comparing abundances from minor ionization stages is probably a risky undertaking.

For the major stages of ionization of different elements in H I regions, i.e., the lowest stages with ionization potentials greater than 13.6 eV, it is generally assumed that nearly all of the atoms are in that stage. This is probably a trustworthy notion for individual regions with hydrogen shielding depths $N(\mathrm{H\ I}) > 10^{19.5}\,\mathrm{cm}^{-2}$, but below this column density

* The rate coefficient $\alpha(X,g)$ also depends on many incidental factors, such as the character and concentration of dust grains, the local density of starlight photons, and the local electron density.

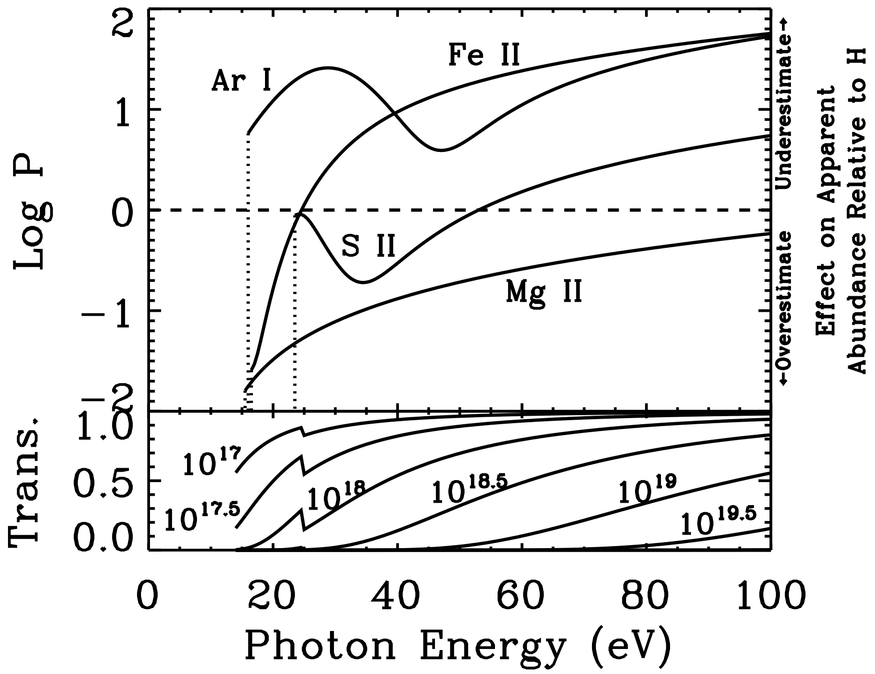

Fig. 1.1. *Top section:* Relative ease of photoionizing Ar, S, Fe, and Mg to ionization stages above the preferred ones (Ar I, S II, Fe II, and Mg II) relative to that of partially ionizing H, expressed in the form of the logarithm of P defined in Eq. 1.3 as a function of the photon energy, under the simplified condition that the radiation field is purely monoenergetic. The amounts by which the derived abundances relative relative to that of H are either underestimated ($\log P > 0$) or overestimated ($\log P < 0$) are defined by Eq. 1.2. Curves for additional elements are shown by Sofia & Jenkins (1998). *Bottom section:* The transmission of photoionizing radiation through different shielding column densities of hydrogen, with the curves labeled according to different values of $\log N$(H I).

photons with energies $< 100\,\mathrm{eV}$ can penetrate the region, as illustrated in the bottom section of Figure 1.1. Once this happens, some fractions of both the element in question and the accompanying hydrogen can be elevated to higher stages of ionization, but by different amounts. It follows that a comparison of an element's most abundant stage to that of H I could lead to a misleading abundance ratio, which differs from the true one by a logarithmic difference

$$\log\zeta(X) - \log\zeta(\mathrm{H}) = \log\left[\frac{1+\frac{n(e)}{n(\mathrm{H})}}{1+P(X)\frac{n(e)}{n(\mathrm{H})}}\right] , \tag{1.2}$$

where

$$\zeta = (\text{preferred stage})/(\text{total}) \quad \text{and} \quad P(X) = \left[\frac{\Gamma(X)\alpha(\mathrm{H})}{\Gamma(\mathrm{H})\alpha(X)}\right] . \tag{1.3}$$

These equations are discussed in more detail by Sofia & Jenkins (1998)*, who also present their more complex modified forms that account for the additional effects of charge exchange with hydrogen. Alterations arising from charge exchange can be very important for certain elements, such as N and O, which have large reaction rate coefficients (Field & Steigman 1971; Butler & Dalgarno 1979).

The curves for $\log P$ for several elements are shown in Figure 1.1. This figure illustrates that under conditions of partial ionization, N(Ar I)/N(H I) underestimates the true value of Ar/H because Ar is more easily ionized than H, while the converse is true for N(Mg II)/N(H I). At first glance, S might appear to be more immune to ionization corrections because its $\log P$ is not far from zero. However, the second ionization potential of S is 23.4 eV, i.e., far above the 13.6 eV needed to ionize hydrogen. Thus, there is some danger that significant amounts of S II could arise from a fully ionized H II region in front of a target star, and this might increase the apparent abundance of S II over that which should have been identified with an H I region under study. To illustrate how important this effect can be, we note that for the extreme case of β CMa the ratio of foreground S II to H I is 10 times solar (Jenkins, Gry, & Dupin 2000).

The picture just presented is an oversimplification, but one that is instructive. In real life, the incident radiation has a distribution of fluxes over different energies, and it is scattered and attenuated by different amounts as deeper layers of a cloud are penetrated. What we view is the composite absorption produced by these layers. One popular approach for calculating these effects is to use the program CLOUDY (Ferland et al. 1998), which is designed to evaluate the various ion fractions at different locations within a cloud that is irradiated from the outside. This program has been made generally available to the public (http://www.nublado.org) and is continuously updated. Another complication is that in some circumstances anomalously large temperatures created by shock heating may lead to collisional ionization, which can elevate even further the populations of high-ionization states (Trapero et al. 1996).

Useful general discussions of the effects that can arise from a mixture of ionized and neutral regions are given by Sembach et al. (2000). It is clear that they are especially important in low-density gases within about 100 pc of the Sun (Jenkins et al. 2000; Jenkins, Gry, & Dupin 2000; Gry & Jenkins 2001). Howk & Sembach (1999) point out the dangers inherent in deriving abundances in damped Lyα systems, and they back up their cautions by noting that the velocity profiles of Al III are very similar to those from species that are expected to arise from H I regions. The notion that such systems may have a considerable amount of partially ionized gas is reinforced by the findings of Vladilo et al. (2003) who noted that Ar I seems to be deficient relative to other α-capture elements that are not expected to be appreciably depleted onto dust grains (see §1.3 below). By definition, damped Lyα systems have column densities $\log N(\text{H I}) > 20.3$, well in excess of the limit $\log N(\text{H I}) = 19.5$ for shielding out photons with $E \lesssim 100\,\text{eV}$. Perhaps these systems are either (1) subjected to appreciable fluxes with $E > 100\,\text{eV}$, (2) are made up of many thinner regions that are each separately exposed to the ionizing radiation, or (3) have strong sources of internal ionization arising from rapid star formation.

* Sofia & Jenkins refer to ζ as δ, but δ is not adopted here because δ has often been used in much of the literature to denote a depletion factor, as expressed here in Eq. 1.4.

1.3 Depletions of Free Atoms onto Dust Grains

1.3.1 Basic Premise

The fact that appreciable fractions of some elements in the ISM have condensed into solid form is supported by a number of independent observations. First, starlight is absorbed and scattered by dust particles or very large molecules—the opacity takes the form of continuous attenuation in the visible and UV, together with discrete absorption bands (2200 Å feature, diffuse interstellar bands in the visible, and infrared absorption features). When compared with the amount of hydrogen present, the magnitude of the attenuation indicates that the proportions of some atoms in solid form are large (see the review by Draine 2004). Second, it is clear from circumstellar emissions in the infrared that many types of evolved stars cast off their dusty envelopes into the ISM. While such dust probably does not account for most of the material that is in solid form within the general ISM, it probably provides nucleation sites for further growth in dense clouds. Finally, we may compare interstellar atomic abundances with solar (or stellar) abundances in the Galactic disk and surmise that the inferred depletions measure the fractional amounts of material hidden in some kind of solid form (or within large molecules that are difficult to identify spectroscopically). Specifically, we may define a depletion of free atoms using the usual bracket notation,

$$[X/\mathrm{H}] = \log(N(X)/N(\mathrm{H})) - \log(X/\mathrm{H})_{\odot} \tag{1.4}$$

and the amount of an element locked up in solids, relative to H, is

$$(X/\mathrm{H})_{\mathrm{dust}} = (X/\mathrm{H})_{\odot}(1 - 10^{[X/\mathrm{H}]}) \ , \tag{1.5}$$

assuming that solar abundances are good reference values that truly reflect the total abundances (see the second footnote in §1.3.3). Much of the discussion that follows in this paper concentrates on the findings on depletions, ones that are strikingly evident from the UV absorption data, but which have also been evident even from the visible absorption lines of Ti II (Wallerstein & Goldsmith 1974; Stokes & Hobbs 1976; Stokes 1978) and the features of Ca II (Snow, Timothy, & Seab 1983; Crinklaw, Federman, & Joseph 1994) (notwithstanding the inherent difficulties in dealing with the uncertainties of the ionization equilibrium of the latter; see Eq. 1.1).

1.3.2 General Properties of the Depletion Trends

To obtain a better understanding of the underlying causes of the depletions of free atoms in space and the various factors that are influential, it is important to identify systematic effects that occur from one element to the next and from one environmental factor to the next. Three important effects have been observed:

(1) Elements that reside within refractory compounds are more severely depleted than ones that mostly condense into volatile ones. Field (1974) was the first to identify this effect by comparing the depletions of different elements toward ζ Oph with their condensation temperatures, defined according to the temperature at which some fixed proportion of an element in a gaseous cosmic mixture freezes out into some solid compound(s). The interpretation offered by Field was that in cooling and expanding mass loss outflows from stars, the dense, inner zones of the flows gave rise to nearly complete depletions of elements making up the refractory compounds, whereas the outer, less dense zones that were cool enough to freeze

out more volatile substances could not fully complete the process. While this is an attractive concept, we must also acknowledge that condensation temperatures are an indication of general strengths of chemical bonds and may thus also apply to the balance of creation and destruction of dust grains in the general ISM (Cardelli 1994). A more modern presentation of the correlations of depletions with condensation temperature (again for ζ Oph) is shown in Figure 4 of the review article by Savage & Sembach (1996).

(2) The strengths of depletions decrease for gas moving at large velocities relative to the undisturbed material in a given region. This effect was first pointed out by Routly & Spitzer (1952) who compared lines of Ca II to those of Na I, and it has been substantiated in greater detail by Siluk & Silk (1974), Vallerga et al. (1993), and Sembach & Danks (1994). Misgivings that this effect could arise from changes in ionization have been overcome by the ultraviolet data (Jenkins, Silk, & Wallerstein 1976; Shull, York, & Hobbs 1977), where several ionization stages for certain elements could be observed. The interpretation of this effect is that gas at high velocities was recently subjected to a shock that was strong enough to partly (or completely) destroy the grains (Barlow 1978a, b; Draine & Salpeter 1979; Jones et al. 1994; Tielens et al. 1994).

(3) The strengths of depletions scale in proportion to the average density of gas (i.e., N(H) divided by distance) along a line of sight (Savage & Bohlin 1979; Harris, Gry, & Bromage 1984; Spitzer 1985; Jenkins, Savage, & Spitzer 1986; Jenkins 1987; Crinklaw et al. 1994). Such a measure is a very crude indication of conditions, since there is no way to discriminate between very compact clouds with high densities and a small filling factor from far more extended regions having only moderately high densities but large filling factors. Nevertheless, the trend supports the propositions that the growth of dust grains is markedly enhanced in dense regions and/or that within these regions the destructive effects of shocks are muted. Successful alternative ways to gauge the predisposition for elements to deplete include the fraction of hydrogen in molecular form (Cardelli 1994) and, toward very distant sources at high Galactic latitudes, simply N(H I) (Wakker & Mathis 2000).

1.3.3 A Reinvestigation of the Depletion Trends

Seven years ago, Savage & Sembach (1996) summarized the interstellar abundances derived from observations using the GHRS instrument aboard *HST*. Since that time, the continued success of *HST* (with the STIS instrument that replaced GHRS) and emergence of *FUSE* have enabled a significant number of important new surveys of interstellar abundances to be carried out. For this reason, it is useful to revisit the general trends, now that a larger suite of results, both new and old, can be compiled and analyzed. Unlike previous studies that directly compared the strengths of depletions of specific elements with tangible properties of the lines of sight (e.g., Jenkins 1987 or Cardelli 1994), we will initially ignore these external factors and instead characterize depletions simply to arise as the result of some measure of each element's general propensity to deplete, which works in combination with an index F_* for the overall strength of depletions (applied to all elements) along the line of sight to a star. This method has the advantage that links in the depletions from element to element are evaluated directly. As a result, they are not weakened by the inevitable inaccuracies in the relationships between individual depletions and some independently measured quantity (either average density or the fraction of H_2). After values of F_* have been defined for many different stars, we can then probe how they correlate with the average density (or any other interesting attribute for a line of sight). When we investigate

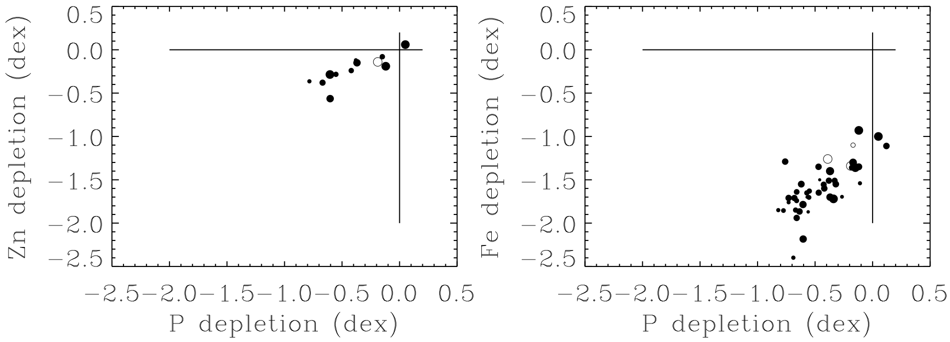

Fig. 1.2. Two comparisons of depletions of pairs of elements along different lines of sight: *Left panel:* Zn vs. *P* and *Right panel:* Fe vs. P. Points with large diameters represent determinations with small errors; open circles apply to cases where $\log N(\mathrm{H}) < 19.5$, where ionization effects may be important (see §1.2).

how depletions change under different conditions, we enjoy the benefit of being able to draw upon a wide selection of examples and not just those for a single element.

For the study presented here, abundances toward 144 stars were identified from over 70 investigations reported in the literature (far too numerous to cite here). The targets were limited to those for which we can extract reliable measures of hydrogen in the form of neutral atoms and H_2, derived from measurements of the Lyα damping profiles and the H_2 Lyman and Werner bands.* Since it is usually impossible (or very difficult) to identify the amounts of hydrogen associated with individual velocity components along a line of sight (without applying simplifying assumptions arising from "undepleted" species), only total column densities over all components were considered. Exceptions to this principle could be made for a few cases where one component strongly dominated the total.

We begin with the simplest assumption that from one line of sight to the next, the depletions of different elements scale with each other in some fixed proportion, as is illustrated for Zn and P shown in the left-hand panel of Figure 1.2. However, this simple prediction does not hold for all elements, as one can see for the case of Fe and P in the right-hand panel of this figure. This behavior seems likely to be explained by the concept that typical dust grains have a mantle that is easily created and destroyed in the ISM, and that this mantle surrounds a relatively indestructible core that survives all but the most energetic (and very rare) shock events (Spitzer 1985; Jenkins, Savage, & Spitzer 1986; Joseph 1988; Spitzer & Fitzpatrick 1993). We are thus forced to consider at least three parameters for a general law that characterizes the depletion of an element X,

$$[X/\mathrm{H}] = A_X F_* + A_{0,X}, \tag{1.6}$$

where A_X represents the relative ease with which an element's individual depletion changes as the general line-of-sight depletion multiplier F_* varies, and $A_{0,X}$ represents an offset attributable to special compounds within the most rugged portions of the grains. For the study

* In some instances, definite determinations for $N(\mathrm{H}_2)$ were not available. However, when upper limits for $N(\mathrm{H}_2)$ were known to be smaller than $0.02N(\mathrm{H\ I})$, we could disregard the effect of H_2 in increasing the value of $N(\mathrm{H_{total}}) = N(\mathrm{H\ I}) + 2N(\mathrm{H}_2)$. Also, based on general findings for H_2 (Savage et al. 1977; Rachford et al. 2002), it is safe to ignore H_2 if the star's $B-V$ color excess is less than 0.1, or (equivalently) $\log N(\mathrm{H\ I}) < 20.3$.

Table 1.1. *Best-fit Depletion Constants*

Elem. X	$\text{Abund}_\odot$ (H = 12)	A_X ($\pm 1\sigma$ error)	$A_{0,X}$ ($\pm 1\sigma$ error)	χ^2	d.f.	Probability of a Worse Fit
C	8.39	-0.097 ± 0.208	-0.148 ± 0.189	2.2	6	0.899
N	7.93	-0.060 ± 0.075	-0.080 ± 0.043	27.9	15	0.022
O	8.69	-0.089 ± 0.067	-0.050 ± 0.052	38.7	28	0.086
Mg	7.54	-0.861 ± 0.046	-0.248 ± 0.026	42.9	62	0.969
Si	7.54	-1.076 ± 0.122	-0.223 ± 0.033	5.0	7	0.660
P	5.57	-0.967 ± 0.055	0.088 ± 0.028	31.9	52	0.987
Cl	5.27	-0.950 ± 0.108	0.300 ± 0.068	41.3	35	0.215
Ti	4.93	-2.226 ± 0.108	-0.844 ± 0.064	30.5	32	0.543
Cr	5.68	-1.373 ± 0.066	-0.854 ± 0.036	16.8	12	0.158
Mn	5.53	-0.685 ± 0.045	-0.774 ± 0.025	52.7	59	0.704
Fe	7.45	-1.198 ± 0.045	-0.950 ± 0.023	59.7	54	0.275
Ni	6.25	-1.440 ± 0.088	-0.917 ± 0.046	31.0	9	0.000
Cu	4.27	-0.408 ± 0.223	-0.974 ± 0.204	7.7	9	0.561
Zn	4.65	-0.522 ± 0.083	0.042 ± 0.053	12.6	12	0.399
Kr	3.23	-0.178 ± 0.134	-0.116 ± 0.104	3.1	9	0.961

presented here, the normalization of F_* was defined to make a value of 1.0 equal to the depletions on line of sight toward ζ Oph, a star that shows for one of its velocity components a significant amount of depletion. It is also a case that has probably received the most attention of any star for depletions of a broad range of different elements [see Table 5 of Savage & Sembach (1996) for a summary].

Weighted least-squares determinations for the constants A_X and $A_{0,X}$ associated with all of the elements covered in this study† are given in Table 1.1. Figure 1.3 shows plots of the observed depletions as a function of F_*; in each case a dashed line is drawn to show the relationship expressed by Equation 1.6 for the appropriate values of A_X and $A_{0,X}$ shown in the table. Within the uncertainties of A_X, the elements C, N, O, and Kr all have slopes that are consistent with zero, in accord with the findings of Cardelli et al. (1996), Meyer, Cardelli, & Sofia (1997), Meyer, Jura, & Cardelli (1998) and Cartledge, Meyer, & Lauroesch (2004). Table 1.1 also indicates the values of χ^2 for the fits, the associated degrees of freedom (d.f. equal to the number of cases minus 2), and the probability of obtaining a worse value of χ^2 assuming that the errors are accurate and a linear fit of the depletions $[X/\mathrm{H}]$ to F_* is a correct model. Values of these probabilities that are unreasonably close to 0 or 1 probably reflect unrealistically large or small errors assigned by the investigators. An exception is Cl, which seems to exhibit a genuinely poor linear relationship.

† Initially, the elements S, Ar, and Ge were also considered, but there were too few cases that met the acceptance criteria to produce meaningful determinations of the depletion parameters. Reference abundances are shown in column 2 of Table 1.1 and were taken from the compilation by Anders & Grevesse (1989), except for the revised solar abundances of C (Allende Prieto, Lambert, & Asplund 2002), N, Mg, Si, Fe (Holweger 2001), and O (Allende Prieto, Lambert, & Asplund 2001). The revised solar abundances appear to have resolved some outstanding discrepancies that appeared to arise between the B-star abundances and the solar ones (Sofia & Meyer 2001), which led to large ambiguities in $[X/\mathrm{H}]$ and $(X/\mathrm{H})_{\mathrm{dust}}$ (Snow & Witt 1996).

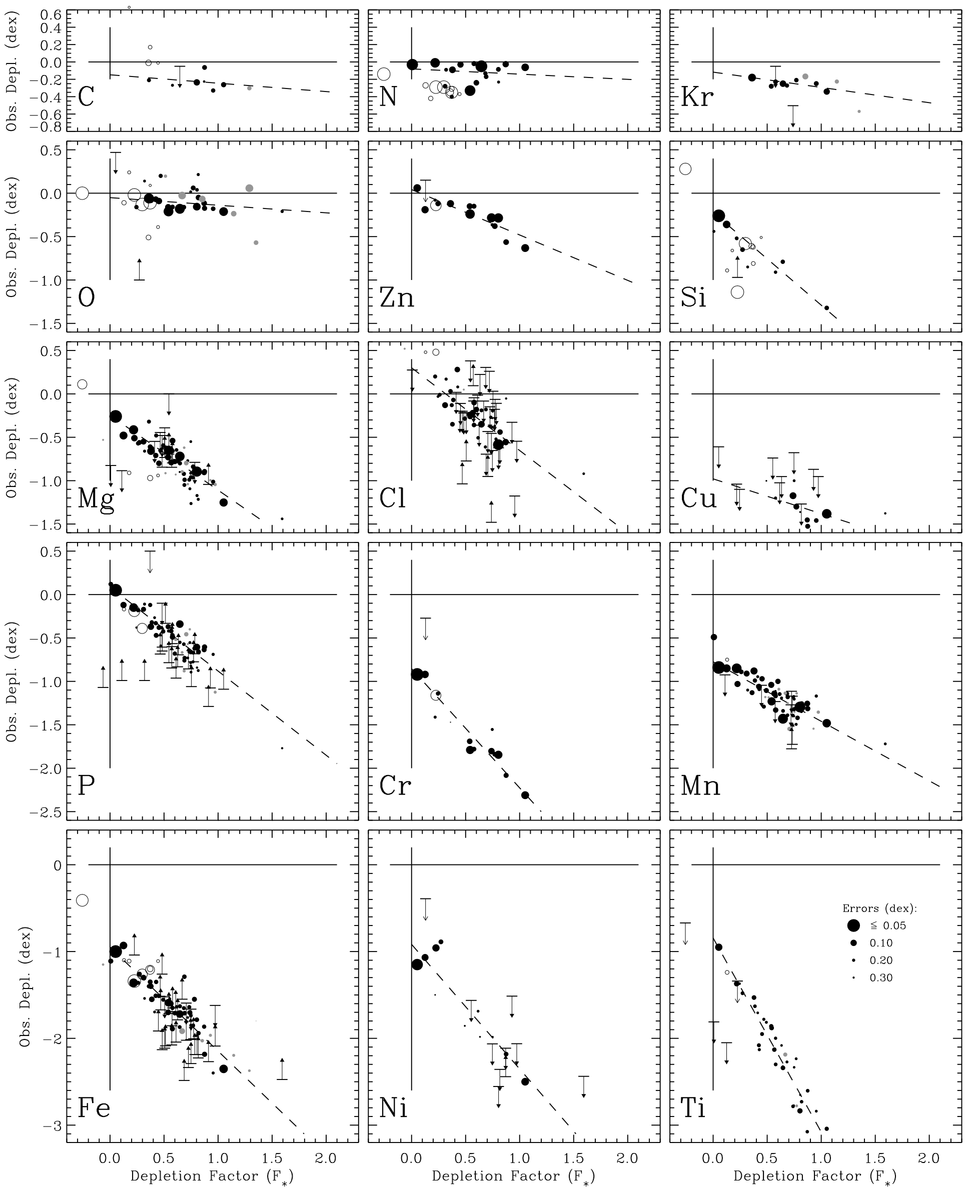

Fig. 1.3. Observed element depletions as a function of the line-of-sight depletion multiplier F_*. In each case, the dashed line represents the linear fit defined by Eq. 1.6 with the constants A_X and $A_{0,X}$ listed in Table 1.1. Cases excluded in the best-fit determinations of these constants include upper and lower limits (arrows) and those with $\log N(\mathrm{H_{total}}) < 19.5$ (open circles). Errors in the observations are designated by the sizes of the symbols (smaller symbols represent less certain results), according to the legend in the lower right panel. Cases for which fewer than three other elements were available to establish a measure of F_* are shown in gray rather than black. The open circles with negative F_* correspond to β CMa, which has an extraordinarily large fraction of ionized gas in front of it (Gry, York, & Vidal-Madjar 1985; Jenkins, Gry, & Dupin 2000).

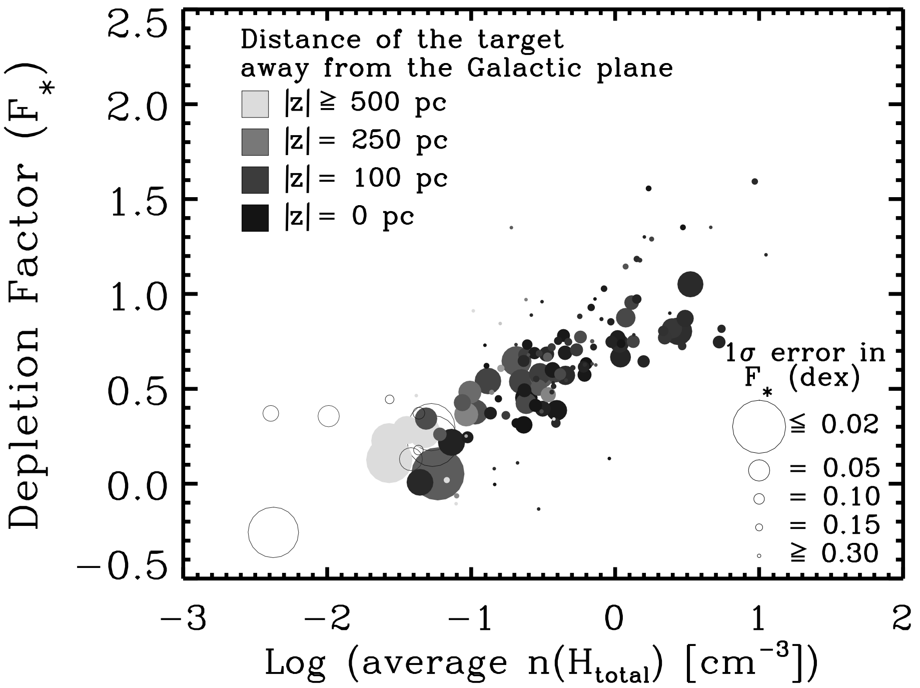

Fig. 1.4. Relationship between the depletion factors F_* toward different stars and their respective average hydrogen densities along the lines of sight. Large symbols are more reliable than small ones, as indicated by the legend in the lower right-hand corner, either because more elements were sampled or the errors in the column densities were smaller. Open circles denote cases where ionization corrections might be important because $\log N(\mathrm{H\ I}) < 19.5$. The darknesses of the filled symbols indicate the target star's distance above or below the Galactic plane.

Figure 1.4 shows how well the values of F_* correlate with the average hydrogen densities along the lines of sight. There is a clear trend between the two, which substantiates the statements made earlier in §1.3.2 (point nr. 3). The lack of any apparent separation between the darker and lighter shaded points indicates that for this sample, there is no clear effect that distinguishes paths toward stars in the lower halo from those well within the Galactic plane (but see §1.5.1).

Savage & Sembach (1996) summarized depletions of the elements Mg, Si, S, Mn, Cr, Fe, and Ni in terms of broad categories that were labeled "warm disk" and "cool disk," in addition to identifying circumstances that included some gas arising from the Galactic halo (see their Table 6). As a point of reference, if one takes their listed depletions and evaluates the corresponding values of F_* for all of the elements*, the warm disk gas is equivalent to $F_* = 0.21$ while the cool disk material is equivalent to $F_* = 0.99$. The rms dispersion of

* For Mg, one should raise the Mg abundances listed by Savage & Sembach by 0.29 dex, in recognition of the improved f-values of the 1240 Å doublet determined by Fitzpatrick (1997). Likewise, abundances of Ni should be increased by 0.27 dex (Fedchak & Lawler 1999)

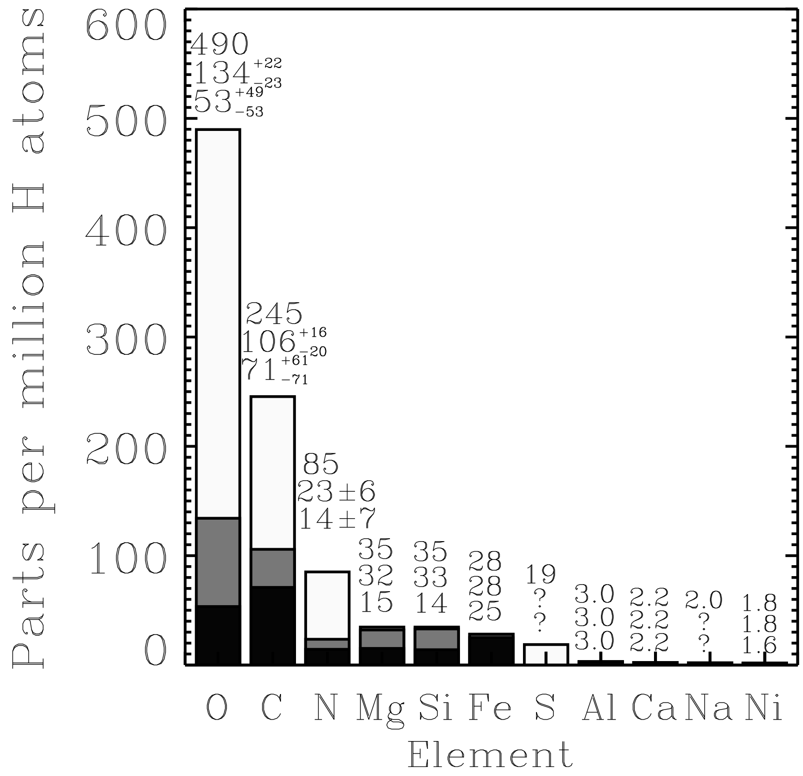

Fig. 1.5. Depictions of elements having solar abundances greater than 10^{-6} times that of H (excluding H and the noble gases He and Ar), with the horizontal positions arranged according to the ranks in total abundances shown by the heights of the bars. The interior of each bar is broken down by the element's fraction in gaseous form (upper, clear portion) and solid form $(X/\mathrm{H})_{\rm dust}$ evaluated from Eqs. 1.5 and 1.6 according to whether $F_* = 1.0$ (gray plus black lower portions) or $F_* = 0.0$ (only the black portion). Numbers over each bar state the values (and errors, if more than 3 ppm) corresponding to the tops of the black, gray and clear zones.

these two numbers from one element to the next is 0.05. From strong deficiencies of Al III compared to S III along certain lines of sight, Howk & Savage (1999) concluded that dust grains reside within ionized regions as well.

1.4 Insights on the Composition of Interstellar Dust

As an aid to help us visualize the composition of dust grains, Figure 1.5 indicates what fractions of the more abundant elements exist in the simplest characterizations of (1) resilient grain cores depicted by the lower, black portions of the bars, (2) the outer, somewhat interchangeable forms (sometimes in mantles and other times as free atoms) shown by the gray extensions, and (3) atoms perpetually in free gaseous form shown by the clear portions that extend to the top of each bar (with a length equal to the total abundance). The divisions between the three zones are based on evaluations of Equation 1.6 for $F_* = 1.0$ (tops of the gray zones) and $F_* = 0.0$ (the boundary between the gray and black zones). The presumption here is that these two values of F_* offer good representations of the quantities of material found in grains that are, respectively, either stripped or well nourished. Note from a previous statement in §1.3.3 that it is not clear from the observations that C, N, and O show significant changes in depletion as F_* progresses from one extreme to the other, so in truth the differences between the gray and black zones are not well established. Two elements shown in the figure were not studied here, primarily because there were problems with the ionization effects discussed in §1.2: Na is seen only as Na I (an unfavored stage of ionization) in the visible, and significant contributions of S II may arise from H II regions. Sofia et al. (1994), Spitzer & Fitzpatrick (1993), and Fitzpatrick & Spitzer (1994) have considered the possible mix of compounds in grains that were consistent with the observed depletions; the current state of this topic is reviewed by Draine (2004).

1.5 Outside the Galactic Plane

1.5.1 Lower Halo

In order to study the composition of gases in the lower halo, it is necessary to eliminate the inevitable foreground contributions arising from material in the Galactic disk. This can be accomplished by selecting velocity components that are displaced from that of the local gas by virtue of either differential Galactic rotation or special kinematics (usually infall, as with material that is often referred to as "intermediate velocity clouds"*). However, in this circumstance it is difficult to obtain useful information on the amount of hydrogen that accompanies this gas. That is, N(H I) derived from the Lyα damping wings applies to all of the hydrogen present, regardless of velocity. Measures of 21-cm emission show hydrogen as function of velocity, but the results are often not very satisfactory because the radio beam covers a solid angle in the sky that is much larger than a typical cloud size and thus may detect material that is not on top of the source viewed in the UV. Also, some of the signal may arise from hydrogen beyond the target if it is a halo star and not a distant QSO or AGN.

One method of overcoming the lack of good information on hydrogen is to use some other element as a proxy, preferably one that is known to be very lightly depleted. For instance, Sembach & Savage (1996) summarized the abundances of various elements relative to the corresponding amounts of Zn in halo gas components along various sightlines. Those findings are reproduced in Table 1.2 in the form of a value followed by the observed dispersion of results from one halo star to the next. For comparison, the table also shows similar ratios for disk gas at two extremes for the depletion index, $F_* = 0.0$ and 1.0.

We must be cautious when interpreting the data shown in Table 1.2. The column densities of Zn II typically indicate that $\log N(\text{H I}) \approx 19.5$, which means that some of the gas could be partially photoionized, and this in turn would indicate that the column density comparisons may be subject to the ionization corrections discussed in §1.2. Nevertheless, even with the possibility that the apparent abundances may be perturbed in this manner, we can still formulate some useful conclusions. For instance, we note from Figure 1.1 that Fe II is more easily ionized to higher stages than Mg II, regardless of the characteristic photon energy. However, according to the entries in Table 1.2, $[\text{Fe}/\text{Zn}]_{\text{halo}} > [\text{Fe}/\text{Zn}]_{\text{disk}}$, while $[\text{Mg}/\text{Zn}]_{\text{halo}} \approx [\text{Mg}/\text{Zn}]_{\text{disk}}$ for $F_* = 0.0$. It is therefore safe to say that Fe is liberated from

* Not to be confused with the high velocity clouds discussed in §1.5.2.

Table 1.2. *Abundances Compared to Zn for Halo and Disk Gas*

Ratio	Halo Value	rms Dispersion	Disk with $F_* = 0.0$	Disk with $F_* = 1.0$
[Mg/Zn]*	–0.23	< 0.19	–0.29	–0.63
[Si/Zn]	–0.26	0.14	–0.27	–0.82
[S/Zn]	–0.05	0.14	...	...
[Cr/Zn]	–0.51	0.13	–0.90	–1.75
[Mn/Zn]	–0.61	0.09	–0.82	–0.98
[Fe/Zn]	–0.64	0.04	–0.99	–1.67
[Ni/Zn]*	–0.56	0.07	–0.96	–1.88

* As noted in an earlier footnote, the originally quoted abundances of Mg and Ni have been increased by 0.29 and 0.27 dex, respectively.

dust grains more easily in the halo than in the disk, regardless of the strength of the ionization (or the value of F_* adopted for the disk gas). Evidently, in the halo the amount of residual iron left in grain cores is not as large as in the most lightly depleted gas in the disk, i.e., $[\mathrm{Fe/H}]_{\mathrm{halo}} > A_{0,Fe} = -0.95$. This effect might arise from the condition that much of the gas in the halo was heavily shocked as it was ejected from the disk and thus the grains were more completely destroyed, or, alternatively, that perhaps ejecta from Type Ia supernovae in the halo have had a chance to enrich the Fe in a time that is shorter than the circulation time between the disk and halo (Jenkins & Wallerstein 1996).

1.5.2 High-velocity Clouds

We now move on to examine the abundances in distinct cloud complexes at high Galactic latitudes that are moving at extraordinarily large velocities (Oort 1966; Mathewson, Cleary, & Murray 1974), i.e., with kinematics clearly not associated with differential Galactic rotation. A current and very comprehensive review of this material has been presented by Wakker (2001). Here, our objective is not to assume some reference abundances and then study the condensation into dust grains, but instead, we seek to use abundances as a tool to gain a better understanding about the origin and history of the material. However, we must still apply the concepts that we have considered earlier and account for the alterations caused by ionization effects and the removal of atoms as they condense into dust grains.

For sightlines that penetrate through well-known high-velocity cloud complexes called Complex C and the Magellanic Stream, Table 1.3 lists the observed deficiencies of the dominant ion X_i of element X in H I regions with respect to neutral hydrogen,

$$[X_i/\mathrm{H\,I}] = \log\{N(X_i)/N(\mathrm{H\,I})\} - \log(X/\mathrm{H})_\odot, \tag{1.7}$$

from which one may define a true depletion of the element

$$[X/\mathrm{H}] = [X_i/\mathrm{H\,I}] + \log\{f(\mathrm{H\,I})/f(X_i)\} \tag{1.8}$$

if the ion ratio $f(\mathrm{H\,I})/f(X_i)$ can be calculated. Tripp et al. (2003) argue that for the Complex C gas in front of 3C 351 the corrections of Equation 1.8 are substantial and are most likely to arise from collisional ionization. The last row of Table 1.3 shows the element

Table 1.3. *Observed Abundance Ratios in the Magellanic Stream (MS) and Complex C (C)*

Object	[N I/ H I]	[O I/ H I]	[S II/ H I]	[Si II/ H I]	[Fe II/ H I]	[Ar I/ H I]	log N(H I)	Refs.
Fairall 9 (MS)	...	...	−0.6	> −1.2	...	...	19.97	[1,2]
NGC 3783 (MS)	> −1.9	...	−0.6	−0.8	−1.5	< −0.2	19.90	[3,4]
Mrk 279 (C)	< −1.2	−0.5	−0.3	−0.4	−0.8	< −0.9	19.49	[5,6]
Mrk 290 (C)	...	...	−1.1	> −1.6	...	...	19.96	[5,7]
Mrk 817 (C)	< −1.4	−0.5	−0.4	−0.5	−0.6	< −1.1	19.48	[5,6]
Mrk 876 (C)	−1.4	...	...	−0.2	−0.4	< −0.9	19.37	[5,6,8]
PG 1259+593 (C)	−1.8	−0.9	−0.8	−0.8	−1.0	−1.24	19.92	[6,9]
3C 351 (C)	< −1.1	−0.7	< 0.1	−0.4	−0.3	...	18.62	[10]
ioniz. corr.	**[N/H]**	**[O/H]**	**[S/H]**	**[Si/H]**	**[Fe/H]**	**[Ar/H]**		
3C 351 (C)	< **−1.4**	**−0.8**	< **−0.3**	**−0.7**	**−0.5**	...		[10]

Key to references: [1] Gibson et al. 2000, [2] Lu, Savage, & Sembach 1994, [3] Lu et al. 1998, [4] Sembach et al. 2001, [5] Gibson et al. 2001, [6] Collins, Shull, & Giroux 2003, [7] Wakker et al. 1999, [8] Murphy et al. 2000, [9] Richter et al. 2001b, [10] Tripp et al. 2003. The values of [O I/H I] listed by Collins et al. (2003) have been adjusted to a reference solar abundance of 8.69 given by Allende Prieto et al. (2001).

abundances after these corrections were made. One can argue that the other four directions through Complex C are probably less susceptible to ionization effects, particularly from photoionization, because their high-velocity gas components have much larger values of N(H I) than that toward 3C 351. While this may be true, the fact that [Ar I/H I] < [O I/H I] for Mrk 279, Mrk 817, and PG 1259+593 warns us that ionization corrections for other elements, while probably small, are not completely inconsequential. (Of all the elements, Ar is the most responsive one to the effects arising from partial photoionization.)

The Complex C determinations shown in Table 1.3 indicate that the generally very mildly depleted species N and O (see §1.3.3) are substantially below their corresponding solar abundances. The findings for O are particularly secure since their corrections arising from Equation 1.8 are very small (e.g., 0.03 dex* for 3C 351), principally because the ionization of O is strongly coupled to that of H through charge exchange reactions that have large rate constants (see §1.2). The fact that N seems even more deficient than O [even after applying the corrections, which amount to < 0.2 dex according to Tripp et al. (2003)] indicates that the gas in Complex C has not only a low metallicity, but it has not undergone multiple generations of secondary element processing that are characteristic of the disk of our Galaxy (Henry, Edmunds, & Köppen 2000). These two considerations disfavor the proposition that Complex C arose from a recent ejection of gas from the Galactic disk, even after some heavy dilution from more pristine material in the Galactic halo or Local Group. Finally, the fact that [Fe/H] is not substantially less than the values for other elements indicates that the fraction of elements locked into grains is much smaller than for gas within the Galactic disk. This finding is consistent with an apparent lack of H_2 for material arising from Complex C in front of PG 1259+593 (Richter et al. 2001a), since H_2 is produced primarily on the surfaces of grains. A question may arise about a possible enhancement of Fe over α-capture elements, but Tripp et al. caution that currently the errors in both the measurements and correction factors are too large to make a sound evaluation of this proposition.

* In Table 1.3 the correction appears to be 0.1 dex, but this is due to roundoff error.

The picture for the Magellanic Stream is not as complete as that for Complex C. Nevertheless, the pattern appears to be very similar, except for evidence that Fe is deficient toward NGC 3783, which in turn suggests that some dust is present [further support for the presence of dust in the Magellanic Stream is suggested by the presence of H_2 (Richter et al. 2001a; Sembach et al. 2001)]. The evidence presented in Table 1.3 is consistent with the picture that the Magellanic Stream is material that has been tidally stripped from the Magellanic Clouds.

1.6 Application to Observations of Abundances Elsewhere

The topics discussed in the preceding sections all lead to interesting insights on the nature of processes that govern the apparent abundances of elements in the gas phase within and near our own Galaxy. A new and exciting frontier is the exploration of abundances in very distant systems (Prochaska, Howk, & Wolfe 2003; Prochaska et al. 2003a, b), once again through the observations of absorption lines against continuum sources (QSOs), but ones at very large redshifts. This is a productive way to understand the chemical state of systems that are otherwise invisible, owing to their great distances. The lessons we have learned from studying the interstellar material in an environment that we know well (our Galaxy) can be applied elsewhere. For instance, we may start with the assumption that the patterns of dust depletion are the same everywhere, regardless of the overall level of metallicity. At the very least, this assumption has been shown to hold true for Galaxy and the LMC by Vladilo (2002). Provided one has measurements of two or more elements with very different indices A_X and $A_{0,X}$, but with somewhat similar production origins and responses to ionization, it should be possible to solve simultaneously the different forms of Equation 1.6 to arrive at a representative F_*. Once this has been done, the F_* and observations of all of the elements may once again be substituted into Equation 1.6 to derive the absolute abundances. These, in turn, lead to our understanding of the chemical histories of such systems, along with key properties of their internal environments.

Acknowledgements. The preparation of this paper was supported by NASA contract NAS5-30110. The author thanks B. T. Draine, J. X. Prochaska, T. M. Tripp, B. D. Savage, and D. Welty for helpful comments on early drafts of this paper.

References

Adams, W. S. 1949, ApJ, 109, 354
Allende Prieto, C., Lambert, D. L., & Asplund, M. 2001, ApJ, 556, L63
——. 2002, ApJ, 573, L137
Anders, E., & Grevesse, N. 1989, Geochim. Cos. Acta, 53, 197
Barlow, M. J. 1978a, MNRAS, 183, 367
——. 1978b, MNRAS, 183, 397
Barlow, M. J., Crawford, I. A., Diego, F., Dryburgh, M., Fish, A. C., Howarth, I. D., Spyromilo, J., & Walker, D. D. 1995, MNRAS, 272, 333
Blades, J. C., Wynne-Jones, I., & Wayte, R. C. 1980, MNRAS, 193, 849
Butler, S. E., & Dalgarno, A. 1979, ApJ, 234, 765
Calura, F., Matteucci, F., Dessauges-Zavadsky, M., D'Odorico, S., Prochaska, J. X., & Vladilo, G. 2004, in Carnegie Observatories Astrophysics Series, Vol. 4: Origin and Evolution of the Elements, ed. A. McWilliam & M. Rauch (Pasadena: Carnegie Observatories, http://www.ociw.edu/symposia/series/symposium4/proceedings.html)
Cardelli, J. A. 1994, Science, 265, 209
Cardelli, J. A., Meyer, D. M., Jura, M., & Savage, B. D. 1996, ApJ, 467, 334

Cartledge, S. I. B., Meyer, D. M., & Lauroesch, J. T. 2004, ApJ, in press (astro-ph/0307182)
Collins, J. A., Shull, J. M., & Giroux, M. L. 2003, ApJ, 585, 336
Cowie, L. L., & Songaila, A. 1986, ARA&A, 24, 499
Crane, P., Lambert, D. L., & Sheffer, Y. 1995, ApJS, 99, 107
Crawford, I. A. 2001, MNRAS, 328, 1115
Crinklaw, G., Federman, S. R., & Joseph, C. L. 1994, ApJ, 424, 748
Draine, B. T. 2004, in Carnegie Observatories Astrophysics Series, Vol. 4: Origin and Evolution of the Elements, ed. A. McWilliam & M. Rauch (Cambridge: Cambridge Univ. Press), in press
Draine, B. T., & Salpeter, E. E. 1979, ApJ, 231, 77
Fedchak, J. A., & Lawler, J. E. 1999, ApJ, 523, 734
Ferland, G. J., Korista, K. T., Verner, D. A., Ferguson, J. W., Kingdon, J. B., & Verner, E. M. 1998, PASP, 110, 761
Field, G. B. 1974, ApJ, 187, 453
Field, G. B., & Steigman, G. 1971, ApJ, 166, 59
Fitzpatrick, E. L. 1997, ApJ, 482, L199
Fitzpatrick, E. L., & Spitzer, L. 1994, ApJ, 427, 232
Gibson, B. K., Giroux, M. L., Penton, S. V., Putman, M. E., Stocke, J. T., & Shull, J. M. 2000, AJ, 120, 1830
Gibson, B. K., Giroux, M. L., Penton, S. V., Stocke, J. T., Shull, J. M., & Tumlinson, J. 2001, AJ, 122, 3280
Gry, C., & Jenkins, E. B. 2001, A&A, 367, 617
Gry, C., York, D. G., & Vidal-Madjar, A. 1985, ApJ, 296, 593
Harris, A. W., Gry, C., & Bromage, G. E. 1984, ApJ, 284, 157
Hartmann, J. 1904, ApJ, 19, 268
Henry, R. B. C., Edmunds, M. G., & Köppen, J. 2000, ApJ, 541, 660
Holweger, H. 2001, in Solar and Galactic Composition, A Joint SOHO/ACE Workshop, ed. R. F. Wimmer-Schweingruber (New York: AIP), 23
Howk, J. C., & Savage, B. D. 1999, ApJ, 517, 746
Howk, J. C., & Sembach, K. R. 1999, ApJ, 523, L141
Jenkins, E. B. 1986, ApJ, 304, 739
——. 1987, in Interstellar Processes, ed. D. J. Hollenbach & H. A. Thronson Jr. (Dordrecht: Reidel), 533
——. 1996, ApJ, 471, 292
Jenkins, E. B., et al. 2000, ApJ, 538, L81
Jenkins, E. B., Gry, C., & Dupin, O. 2000, A&A, 354, 253
Jenkins, E. B., Savage, B. D., & Spitzer, L., Jr. 1986, ApJ, 301, 355
Jenkins, E. B., Silk, J., & Wallerstein, G. 1976, ApJS, 32, 681
Jenkins, E. B., & Wallerstein, G. 1996, ApJ, 462, 758
Jones, A. P., Tielens, A. G. G. M., Hollenbach, D. J., & McKee, C. F. 1994, ApJ, 433, 797
Joseph, C. L. 1988, ApJ, 335, 157
Kimble, R. A., et al. 1998, ApJ, 492, L83
Knauth, D. C., Federman, S. R., & Lambert, D. L. 2003, ApJ, 586, 268
Kondo, Y., Wamsteker, W., Boggess, A., Grewing, M., de Jager, C., Lane, A. L., Linsky, J. L., & Wilson, R. 1987, Exploring the Universe with the IUE Satellite (Dordrecht: Reidel)
Lu, L., Savage, B. D., & Sembach, K. R. 1994, ApJ, 437, L119
Lu, L., Savage, B. D., Sembach, K. R., Wakker, B., Sargent, W. L. W., & Oosterloo, T. A. 1998, AJ, 115, 162
Mathewson, D. S., Cleary, M. N., & Murray, J. D. 1974, ApJ, 190, 291
Merrill, P. W., Sanford, R. F., Wilson, O. C., & Burwell, C. G. 1937, ApJ, 86, 274
Meyer, D. M., Cardelli, J. A., & Sofia, U. J. 1997, ApJ, 490, L103
Meyer, D. M., Jura, M., & Cardelli, J. A. 1998, ApJ, 493, 222
Moos, H. W., et al. 2000, ApJ, 538, L1
Morton, D. C., Drake, J. F., Jenkins, E. B., Rogerson, J. B., Spitzer, L., & York, D. G. 1973, ApJ, 181, L103
Murphy, E. M., et al. 2000, ApJ, 538, L35
Oort, J. H. 1966, BAIN, 18, 421
Pettini, M. 2003, in Cosmochemistry: The Melting Pot of Elements (Cambridge: Cambridge Univ. Press), in press (astro-ph/0303272)
Plaskett, J. S., & Pearce, J. A. 1933, Pub. Dominion Ap. Obs., 5, 167
Prochaska, J. X., Howk, J. C., & Wolfe, A. M. 2003, Nature, 423, 57
Prochaska, J. X., Gawiser, E., Wolfe, A. M., Castro, S., & Djorgovski, S. G. 2003a, ApJ, 595, L9
Prochaska, J. X., Gawiser, E., Wolfe, A. M., Cooke, J., & Gelino, D. 2003b, ApJS, 147, 227
Rachford, B., et al. 2002, ApJ, 577, 221

Richter, P., Sembach, K. R., Wakker, B. P., & Savage, B. D. 2001a, ApJ, 562, L181
Richter, P., Sembach, K. R., Wakker, B. P., Savage, B. D., Tripp, T. M., Murphy, E. M., Kalberla, P. M. W., & Jenkins, E. B. 2001b, ApJ, 559, 318
Rogerson, J. B., Spitzer, L., Drake, J. F., Dressler, K., Jenkins, E. B., Morton, D. C., & York, D. G. 1973a, ApJ, 181, L97
Rogerson, J. B., York, D. G., Drake, J. F., Jenkins, E. B., Morton, D. C., & Spitzer, L. 1973b, ApJ, 181, L110
Routly, P. M., & Spitzer, L. 1952, ApJ, 115, 227
Savage, B. D., & Bohlin, R. C. 1979, ApJ, 229, 136
Savage, B. D., Bohlin, R. C., Drake, J. F., & Budich, W. 1977, ApJ, 216, 291
Savage, B. D., & Sembach, K. R. 1991, ApJ, 379, 245
——. 1996, ARA&A, 34, 279
Sembach, K. R., & Danks, A. C. 1994, A&A, 289, 539
Sembach, K. R., Howk, J. C., Ryans, R. S. I., & Keenan, F. P. 2000, ApJ, 528, 310
Sembach, K. R., Howk, J. C., Savage, B. D., & Shull, J. M. 2001, AJ, 121, 992
Sembach, K. R., & Savage, B. D. 1992, ApJS, 83, 147
——. 1996, ApJ, 457, 211
Shull, J. M., York, D. G., & Hobbs, L. M. 1977, ApJ, 211, L139
Siluk, R. S., & Silk, J. 1974, ApJ, 192, 51
Snow, T. P., Timothy, J. G., & Seab, C. G. 1983, ApJ, 265, L67
Snow, T. P., & Witt, A. N. 1996, ApJ, 468, L65
Sofia, U. J., Cardelli, J. A., & Savage, B. D. 1994, ApJ, 430, 650
Sofia, U. J., & Jenkins, E. B. 1998, ApJ, 499, 951
Sofia, U. J., & Meyer, D. M. 2001, ApJ, 554, L221
Spitzer, L. 1985, ApJ, 290, L21
Spitzer, L., & Cochran, W. D. 1973, ApJ, 186, L23
Spitzer, L., Drake, J. F., Jenkins, E. B., Morton, D. C., Rogerson, J. B., & York, D. G. 1973, ApJ, 181, L116
Spitzer, L., & Fitzpatrick, E. L. 1993, ApJ, 409, 299
Spitzer, L., & Jenkins, E. B. 1975, ARA&A, 13, 133
Stokes, G. M. 1978, ApJS, 36, 115
Stokes, G. M., & Hobbs, L. M. 1976, ApJ, 208, L95
Tielens, A. G. G. M., McKee, C. F., Seab, C. G., & Hollenbach, D. J. 1994, ApJ, 431, 321
Trapero, J., Welty, D. E., Hobbs, L. M., Lauroesch, J. T., Morton, D. C., Spitzer, L., & York, D. G. 1996, ApJ, 468, 290
Tripp, T. M., et al. 2003, AJ, 125, 3122
Vallerga, J. V., Vedder, P. W., Craig, N., & Welsh, B. Y. 1993, ApJ, 411, 729
Vladilo, G. 2002, ApJ, 569, 295
Vladilo, G., Centurión, M., D'Odorico, V., & Péroux, C. 2003, A&A, 402, 487
Wakker, B. P. 2001, ApJS, 136, 463
Wakker, B. P., et al. 1999, Nature, 402, 388
Wakker, B. P., & Mathis, J. S. 2000, ApJ, 544, L107
Wallerstein, G., & Goldsmith, D. 1974, ApJ, 187, 237
Weingartner, J. C., & Draine, B. T. 2001, ApJ, 563, 842
Welsh, B. Y., Vedder, P. W., & Vallerga, J. V. 1990, ApJ, 358, 473
Welty, D. E., & Hobbs, L. M. 2001, ApJS, 133, 345
Welty, D. E., Hobbs, L. M., & Kulkarni, V. P. 1994, ApJ, 436, 152
Welty, D. E., Hobbs, L. M., & Morton, D. C. 2003, ApJS, 147, 61
Welty, D. E., Morton, D. C., & Hobbs, L. M. 1996, ApJS, 106, 533
Woodgate, B. E., et al. 1998, PASP, 110, 1183
Young, R. K. 1922, Pub. Dominion Ap. Obs., 1, 219